Lawrence Berkeley National Laboratory
Recent Work

Title

HYDRAULIC AND MECHANICAL PROPERTIES OF NATURAL FRACTURES IN LOW-PERMEABILITY ROCK

Permalink

https://escholarship.org/uc/item/0m8219z7

Author

Pyrack-Nolte, L.J.

Publication Date

1987

Lawrence Berkeley Laboratory
UNIVERSITY OF CALIFORNIA

EARTH SCIENCES DIVISION

To be presented at the Sixth International Conference
on Rock Mechanics, Montreal, Quebec, Canada,
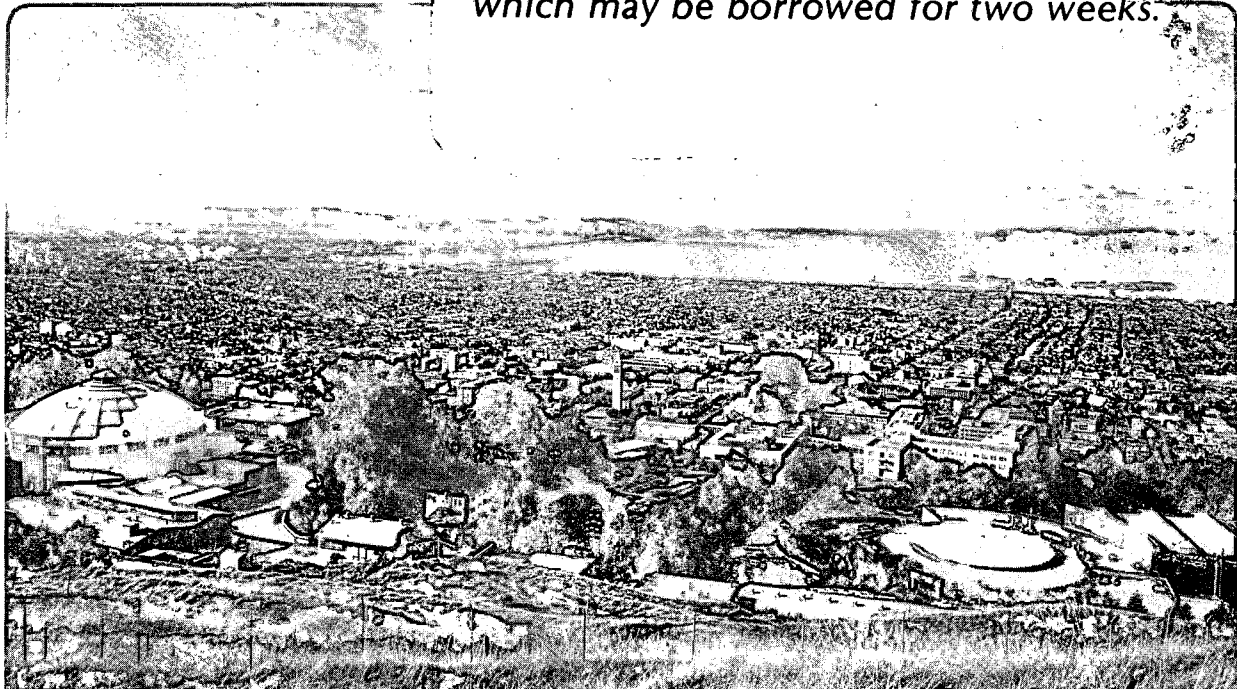August 30-September 3, 1987

HYDRAULIC AND MECHANICAL PROPERTIES OF NATURAL
FRACTURES IN LOW-PERMEABILITY ROCK

L.J. Pyrack-Nolte, L.R. Myer, N.G.W. Cook,
and P.A. Witherspoon

January 1987

DISCLAIMER

HYDRAULIC AND MECHANICAL PROPERTIES OF
NATURAL FRACTURES IN LOW-PERMEABILITY ROCK

Laura J. Pyrack-Nolte, Larry R. Myer, Neville G.W. Cook, and Paul A. Witherspoon

Earth Sciences Division
Lawrence Berkeley Laboratory
University of California
Berkeley, California 94720

January 1987

Laura J. Pyrak-Nolte
Earth Sciences Division, Lawrence Berkeley Laboratory, and
Department of Materials Science and Mineral Engineering, University of California, Berkeley, California

Larry R. Myer
Earth Sciences Division, Lawrence Berkeley Laboratory, and

Neville G.W. Cook
Earth Sciences Division, Lawrence Berkeley Laboratory, and
Department of Materials Science and Mineral Engineering, University of California, Berkeley, California

Paul A. Witherspoon
Earth Sciences Division, Lawrence Berkeley Laboratory, and
Department of Materials Science and Mineral Engineering, University of California, Berkeley, California

ABSTRACT: The results of a comprehensive laboratory study of the mechanical displacement, permeability, and void geometry of single rock fractures in a quartz monzonite are summarized and analyzed. A metal-injection technique was developed that provided quantitative data on the precise geometry of the void spaces between the fracture surfaces and the areas of contact at different stresses. At effective stresses of less than 20 MPa fluid flow was proportional to the mean fracture aperture raised to a power greater than 3. As stress was increased, contact area was increased and void spaces become interconnected by small tortuous channels that constitute the principal impediment to fluid flow. At effective stresses higher than 20 MPa, the mean fracture aperture continued to diminish with increasing stress, but this had little effect on flow because the small tortuous flow channels deformed little with increasing stress.

RESUME: Les résultats d'une étude complète en laboratoire du déplacement mécanique, de la perméabilité, et de la géometrie des vides d'une fracture unique dans un quartz monzonite sont résumés et analysés. Une technique d'injection de métal est présentée, elle fournit des résultats quantitatifs sur l'exacte géométrie des vides compris entre les surfaces de la fracture et les zones d'aspérités en contact. Une augmentation de la contrainte effective entraine une diminution non linéaire de l'ouverture moyenne des vides, et une augmentation non linéaire de la surface de contact moyenne. Sous une contrainte effective de moins de 20 MPa, l'écoulement des fluides est proportionnel à une puissance supérieure à trois de l'ouverture moyenne de la fracture. L'augmentation de la contrainte provoque le changement de la surface de contact, les vides deviennent alors reliés par d'étroits canaux tortueux qui constituent le principal obstacle à l'écoulement. Sous une contrainte effective supérieure à 20 MPa, l'ouverture moyenne de la fracture continue de diminuer avec l'augmentation de contrainte, cela a peu d'influence sur l'écoulement parce que les canaux étroits et tortueux se déforment peu quand la contrainte augmente.

ZUSAMMENFASSUNG: Es werden die Ereignisse eines ausführlichen Laborversuchs sur Bestimmung der mechanischen Derschiebung, der Permeabilität und der Kluftgeometrie einselne Brüche in einem Quars monsonit zusammen gefasst und untersucht. Es wird ein Metalleinspritz-verfahren beschrieben, das in der Lage ist, quantitative Messwerte über die genaue Geometrie des Porenraums zwischen den Bruchflächen und unebenen Kontaktflächen zu liefern. Mit effektivem Druck nimmt die Poren-öffnung in nicht linearem Masse ab und die durchschnittliche Kontaktfläche in nicht linearem Masse zu. Bei effektiven Spannungen von weniger als 20 MPa fliesst die Flüssigkeit proportionel zur mittleren Poren-öffnung zu einem Exponenten grösser als drei. Mit ansteigendem Druck wird die Anzahl der Flächen in Kontakt verändert und Porenräume werden über kleine gewundene Kanäle verbunden, welche das Haupt hindernis für die Flüssigkeit bilden. Bei effektiven Spannungen grösser als 20 MPa verringert sich die mittlere Bruch öffnung weiter mit ansteigender Spannung, aber dies hat wenig Einfluss auf den Fluss, weil die gewundenen Kanäle nur wenig mit ansteigender Spannung verformt werden.

1 INTRODUCTION

Fractures, including joints and faults, are a major concern in the geologic isolation of nuclear wastes in low-permeability rock. Fractures are the principal conduits along which potentially contaminated groundwater can flow in rock masses with low permeability. Knowledge of the mechanical and hydraulic behavior of fractures in low-permeability rock masses is fundamental to the study of nuclear and toxic waste isolation, oil and gas recovery, and fault mechanics.

Fluid flow through fractures in low-permeability rocks depends on the state of stress in the rock mass. A fracture can be thought of as two surfaces in partial contact. When a fracture is stressed, the void space deforms and changes in contact area occur, affecting the hydraulic and mechanical properties of the rock. Several researchers have investigated the displacement of fractures and the increase in contact area as functions of applied normal stress. Goodman (1976) measured the deformation of fractured and whole samples and developed an empirical linear relationship between fracture displacement and the logarithm of effective stress. Goodman suggested that the nonlinear behavior of fracture permeability (which depends on aperture) under stress is accounted for by the nonlinear and inelastic behavior of a fracture under compression. Swan (1983) measured fracture surface topography and normal stiffness in slate joints. For certain conditions and assumptions, he observed that hydraulic conductivity, normal stiffness, and true contact area are simple function of pressure and initial aperture and that the surface roughness properties appear to be irrelevant. Brown and Scholz (1985), however, determined from theoretical and experimental results that fracture displacement is not only a function of the elastic properties of the rock but also depends critically on the way in which the surface topography affects the distribution of contact area.

Measurements of fracture contact area have been made using sheets of pressure-sensitive paper (Duncan and Hancock 1966) and deformable film (Iwai 1976; Bandis et al. 1983). Both methods have shown that contact area increases with applied stress and is dependent on rock type. However, these methods are subject to considerable error, especially when the apertures are smaller than the thickness of the sheet.

Several investigations of fluid flow through single fractures have been carried out in the laboratory under varying conditions. Iwai (1976) studied flow through single induced fractures as functions of displacement, contact area, and stress up to 20 MPa. He found that there is always a residual flow, even at high stresses, and that the cube of the aperture is proportional to flow when corrected by the amount of the residual flow. From an experiment in which the contact area was varied artificially, Iwai determined

that flow decreases hyperbolically as the contact area increases. For real fractures, however, he observed that contact area has a small effect on the flow for some samples but a greater effect in other samples, especially those with apertures less than 15 μm. Gale and Raven (1980) studied the effect of stress on radial fluid flow through natural fractures for samples of various sizes and stresses up to 30 MPa. Finding that their results did not follow the cubic law model, they suggested that the change in contact area with stress plays a major role in decreasing the flow. Kranz et al. (1979) measured the permeability of artificial and induced joints in granite for stresses up to 200 MPa. They observed that permeability is not directly related to effective stress but is a function of confining pressure and pore pressure, each multiplied by a pre-factor that depends on surface roughness of the joint and on ambient pressure. Engelder and Scholz (1981) studied fluid flow along artificial fractures using effective stresses up to 200 MPa. They found that changes in confining pressure have a larger influence than changes in pore pressure and that their data agree well with a "cubic" law modified for variable cross section as a result of applying stress. Walsh (1981) derived a relationship for fluid flow as a function of confining pressure and pore pressure. He concluded that the flow rate is proportional to the product of two factors: tortuosity and aperture. Examining the data of Kranz et al., he observed that the effect of tortuosity could be neglected for fluid flow, since aperture is raised to the third power and dominates the tortuosity term, which is only raised to the first power. In contrast, a theoretical study by Tsang (1984) concludes that tortuosity and surface roughness greatly affect the flow, especially when contact area is greater than 30%.

This brief review points out several inconsistencies, such as the applicability of the cubic law and the effect of void geometry (contact area, tortuosity) on flow. This paper reports the results of experiments and analyses of the hydraulic and mechanical properties of natural fractures as a function of stress and discusses the relationship of these properties to changes in the fracture contact area and void geometry. Hydraulic and mechanical properties of three fractures were measured at effective normal stresses up to 85 MPa. Using a nondestructive metal-injection technique, actual casts of fracture void space were obtained at stresses up to 85 MPa, providing quantitative data on the changes in fracture contact area and void geometry with increasing stress.

2 EXPERIMENTAL PROCEDURE

Tests were performed on three core samples (E30, E32, and E35) of quartz monzonite (Stripa granite) measuring 52 mm in diameter by 77 mm in height. Each sample contained a single natural fracture orthogonal to the long axis of the core. Hydraulic conductivity and mechanical displacement were measured for each of these samples, and changes in fracture void geometry and contact area were evaluated for samples E30 and E32.

A linear flow technique (quadrant flow) was used to measure hydraulic conductivity. In this technique the intersection of the fracture plane with the circumference of the sample is sealed everywhere except along two diametrically opposed quadrants, as shown schematically in Figure 1. A manifold placed on the sample permits fluid to flow through the fracture from one unsealed quadrant to the other. This technique was employed because of sample size; if a radial flow method had been used, the central borehole would have been very small and the results would have reflected the loss of energy predominantly due to flow adjacent to the borehole rather than the loss of energy due to flow through the whole fracture.

A constant effective stress was maintained in the fracture by applying an axial load to the sample in a test machine. An upstream pressure of 0.4 MPa was applied, and flow measurements were made for one complete loading and unloading cycle and an additional loading cycle up to a maximum effective stress of 85 MPa.

Fracture displacement was also measured on the same samples used for fluid flow measurement. Three annular collars were attached to the sample. The inside surface of
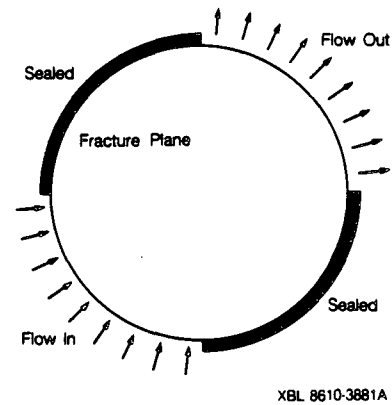

Figure 1. Flow path in quadrant flow technique.

the annulus did not touch the rock surface; each collar was secured to the rock by three pointed screws. The collars were carefully placed to ensure that they were equally separated and parallel. The assembly was placed in the test machine, where axial stresses up to 85 MPa were applied normal to the fracture plane. Four precision linear variable differential transformers (LVDTs, rated repeatability of 1.0×10^{-7} m) were attached in pairs on diametrically opposed sides of the sample. One set of LVDT's spanned the fracture and measured the displacement across both the fracture and the intact rock adjacent to the fracture. The second set measured the displacement of an equal length of the intact rock. The fracture displacement was calculated from the difference between the displacements measured by the first set of transducers and those of the second set. Performance of the measurement system was evaluated by duplicating the experiment using a solid aluminum cylinder of the same dimensions as the rock sample.

A metal injection technique was used to study the fracture void geometry and contact area as a function of stress. The metal used for injection is one of a family of bismuth-lead-tin alloys of which Wood's metal is the most commonly recognized. In the liquid phase, these metals are nonwetting with an effective surface tension of roughly six-tenths that of mercury (Swanson 1979), namely, 0.282 N/m for the Wood's metal. The alloy (Cerrosafe) used in these experiments has a melting point of 160 °F to 190 °F. The Wood's-metal injection technique is similar to mercury porosimetry methods, but it has the advantages of yielding actual metal casts of the voids for the same fracture in experiments at different stresses. These casts can then be studied in detail as described below. Wood's-metal injection techniques have been used by other investigators (Swanson 1979; Yadav et al. 1984) to study the pore geometry of sandstone cores.

For the study of fracture void geometry, the fractured sample was held in a triaxial test vessel maintained at a temperature just above the melting point of the alloy. The vessel was placed in the test machine and an axial load applied normal to the fracture surface. To perform an injection test, the triaxial vessel was evacuated and molten metal pumped into the test vessel until the desired pore fluid pressure was obtained. Both the fluid pressure and the axial load were maintained until the metal in the test vessel had solidified. When the sample was removed from the vessel, the two halves of the sample were separated to reveal metal casts of the void geometry corresponding to the effective stress of the test. Some casts adhere to one surface, some to the other.

The distribution of metal on the two fracture surfaces was examined using both a scanning electron microscope (SEM) and photographic techniques. Images of each of the two fracture surfaces were superimposed to form a composite image of the contact area and void geometry. A Zeiss image analyzer was used in quantitatively evaluating the composite images.

Injections were made on samples E30 and E32 at effective stresses of 3, 33, and 85 MPa.

2

3 RESULTS

Fracture displacements for two complete loading/unloading cycles for one sample (E30) are shown in Figure 2. Though nonlinear, there was very little hysteresis and, within the scatter of the results, no difference in displacement between loading cycles. Deformation of asperities and voids within the fractures must therefore have been elastic. It should be noted that the fracture had been loaded to 85 MPa on several occasions for different tests prior to collection of the data shown in Figure 2. Typically, some hysteresis is observed in the initial loading cycle for natural fractures. However, upon further cycling, hysteresis decreases, and hence so does the difference in displacement between cycles (Bandis et al. 1983; Gale and Raven 1980).

Figure 3 shows fracture displacement versus applied normal stress for the three different fractures, E30, E32, and E35. Though the magnitude of the total displacement varies for the different samples, all the samples exhibit a rapid increase in displacement up to about 10 MPa. Above 10 MPa, the increase in fracture displacement becomes more gradual but does not reach zero, even at 85 MPa. This suggests that even at the highest stresses, numbers of voids must still have been open in all these fractures, least of all for E32 and most of all for E35. The maximum fracture displacement values measured at 85 MPa for samples E30, E32, and E35 are listed in Table 1.

Table 1. Values of experimentally determined displacement at 85 MPa and maximum displacement, d_{max}, determined from equation (1).

Specimen	Displacement at 85 MPa	d_{max}
E32	4.5 μm	6.6 μm
E30	9.5 μm	12.5 μm
E35	28.1 μm	46.0 μm

The inverse of the tangent slopes to the displacement-versus-stress curve is defined as the specific stiffness of the fracture. Values of specific stiffness for these fractures plotted in Figure 4, were determined graphically from the data in Figure 3.

Specific stiffness for all of the samples is nonlinear with stress, in disagreement with the linear relationship assumed by Walsh (1981). Specific stiffness increases rapidly with stress up to about 10 MPa and then increases at a decreasing rate. Though the trend is less pronounced for sample E30, the specific stiffness for these fractures appears to approach a constant value at high stress levels. Ultimately, of course, when all the void spaces between the fracture surfaces close, the specific stiffness must become infinite for each fracture. However, the stresses needed to achieve complete closure would have to be very high.
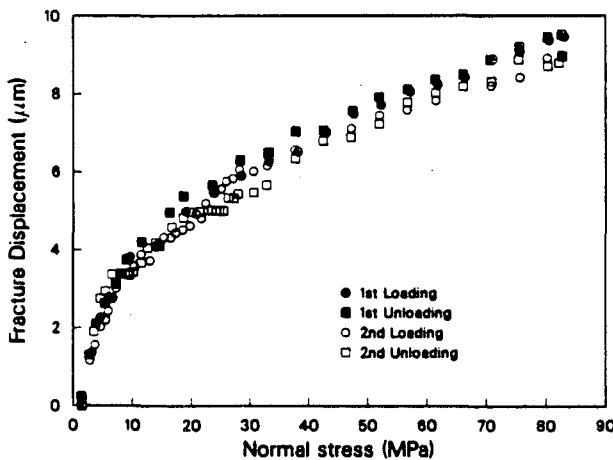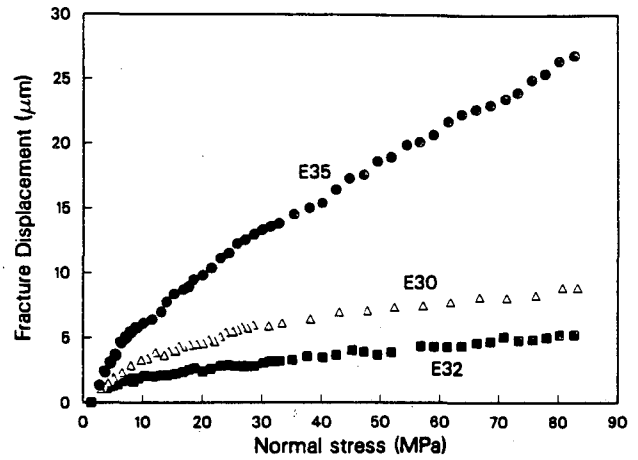

Figure 3. Fracture displacements as a function of normal stress on fracture for samples E35, E30, and E32.

Fracture displacement tests have also been performed on E30 under dry conditions at 100 °C and under saturated conditions at room temperature and at 95 °C. No significant difference in displacement behavior is observed. The difference between the best-fit curves for tests under each of these conditions and that for the test at room-temperature dry conditions is less than one micron at any stress level.

Figure 5 compares fluid flow data for all three samples. Data for E30 and E32 are obtained from the first unloading cycle. Though the magnitude of the flow varies between loading and unloading cycles, the trend of a rapid decrease in flow at low stresses and a much more gradual decrease in flow at higher stresses is observed to be independent of the load cycle. Similar behavior has also been observed in flow measurements made by other investigators (Iwai 1976; Engelder and Scholz 1981; Raven and Gale 1985). Data presented for E35 are obtained from the first loading cycle because that set is the most complete. For samples E30 and E32, a rapid decrease in flow is observed as stress is increased to about 20 MPa. This change in flow corresponds to the rapid increase in fracture closure observed in the displacement measurements. Flow in sample E35 continues to decrease with increasing stress above 20 MPa, whereas the flow for E30 and E32 appears to approach a constant value. The small but finite flow in samples E30 and E32, even at 85 MPa, is significant in that it suggests that flow approaches an irreducible level at high stresses. At these high stresses, mechanical displacement of the fracture continues as demonstrated by the finite values
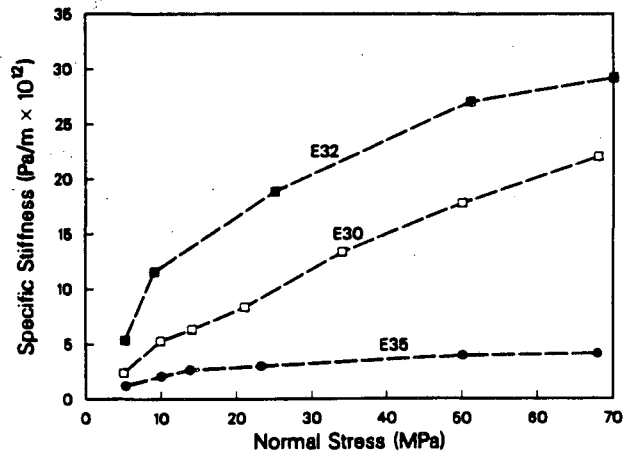

Figure 2. Comparison of fracture displacements for two sequential loading/unloading cycles for sample E30.

Figure 4. Specific stiffness for the three mechanical displacement tests shown in Figure 3.
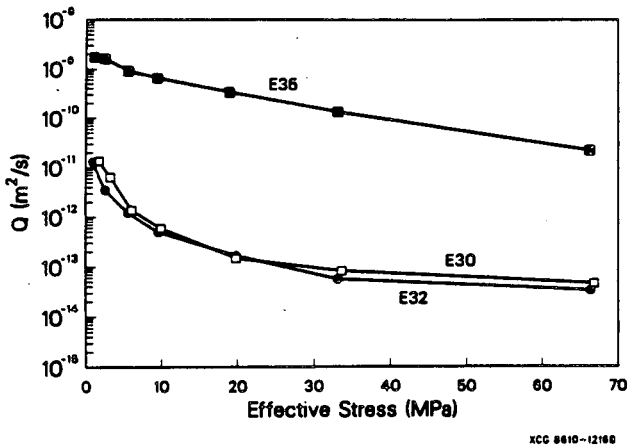
3

Figure 5. Comparison of flow per unit head drop as a function of effective stress for samples E35, E30, and E32.

of specific stiffness (Figure 4). However, this deformation, which must be a result of void closure, has very little effect on the fluid flow for samples E30 and E32. Iwai (1976), and Raven and Gale (1985) have also observed irreducible flow at the highest stresses, even though fracture displacement continued.

In Figure 6, the flow test data are plotted in the conventional format of the logarithm of average fracture displacement versus logarithm of flow. The effect of the irreducible flow is seen as a departure from linearity in this plot. At the lowest values of flow, mechanical displacement continues with virtually no change in the flow. The slope of the linear portion of the curve is not equal to one-third as would be expected if the flow followed the commonly accepted "cubic" law relationship derived for a parallel plate model.

In the analysis of fracture displacement and fluid flow data, a cubic relation is not assumed. Instead, the model consists of a general power relationship between fracture closure and fluid flow as well as a constant term representing the irreducible flow:

$$Q = Q_\infty + C\,(d_{max}-d)^n \qquad (1)$$

where:
  Q = measured value of flow
  Q_∞ = irreducible flow
  C = fitted constant
  d_{max} = maximum value of displacement
  d = measured value of displacement
  n = power relation.

A linear least-squares (Press et al. 1986) fitting routine applied to the logarithm of these quantities in equation (1) is used to determine Q_∞, d_{max}, n and C.
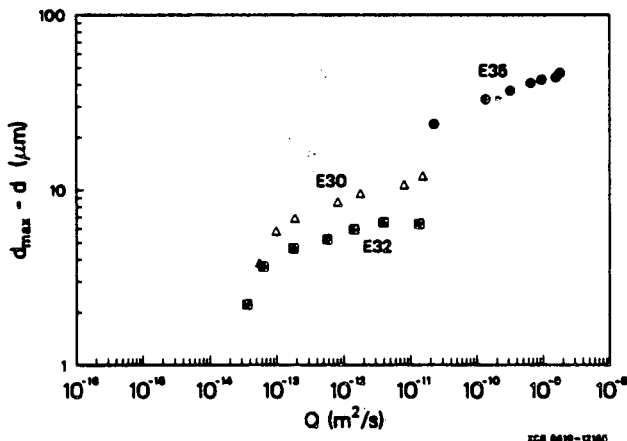
Table 1 lists the measured values of displacement at a stress of 85 MPa and the values of the fitted maximum displacement, d_{max}. Physically, the parameter d_{max} corresponds to the fracture displacement which would result if stress were increased until all voids in the fracture closed. Though obtained by least-squares fitting to flow data, values of d_{max} are plausible when compared to the mechanically measured values at 85 MPa and the slope of the displacement-versus-stress curves. For example, it is plausible that E32, the stiffest fracture, would close to a maximum of 6.6 μm if sufficient stresses were applied, whereas E35, the most compliant fracture could close an additional 20 μm.

When equation (1) is applied to the data, the result, as shown in Figure 7, is a power law relationship between flow and displacement. However, the values of the exponents in equation (1) of 8.3, 9.8, and 7.6, for E30, E32, and E35, respectively, differ greatly from a cubic law representation.

Figure 8 shows composite images made from SEM micrographs of the Wood's metal in the fracture voids of sample E30 at effective stresses of 3, 33, and 85 MPa. Areas of contact are depicted as black areas and the flowpaths are in white. At 3 MPa (Figure 8a), the contact area appears as isolated "islands" in "oceans" of metal. The void area in the fracture is much greater than the contact area and is freely interconnected. The islands of contact area range in size from 5 μm to 0.1 mm. As the stress increases (Figure 8b & 8c), the "islands" of contact areas become "continents," with "lakes" of metal connected by filamentary, tortuous "streams" of metal. Although the lakes of metal may be measured on a scale of millimeters, many of the streams are measured in micrometers. The tortuosity of the interconnected flowpaths (white) is quite noticeable in Figure 8c.

Figure 9 shows composite images of the Wood's metal between the fracture surfaces for samples E30 and E32 for effective stresses of 3, 33, and 85 MPa. Each image in the figure is a composite of two photographs, one of each fracture surface. Areas of contact are white; flowpaths or voids are black. A difference in the shape, size, and distribution of contact area is observed between E30 and E32 at all stresses. Sample E30 possesses many large areas of contact, with more and more smaller areas of contact being generated near these large areas as the stress is increased. The contact areas of E30 tend to be large and clustered, whereas those of E32 are smaller, more numerous, and elongate.

An image analyzer was used to obtain percent contact area at different stress levels for E30 and E32 from the composite images shown in Figure 9. Results are plotted in Figure 10. At 3 MPa, the contact area of sample E30 is about 8%; it increases to about 15% at 33 MPa and to 30% at 85 MPa. For sample E32, the contact area was higher at all stress levels, beginning at about 15% at 3 MPa, increasing to 42% at 33 MPa, and remaining essentially constant at 85 MPa. Greenwood and Williamson (1966) postulated that contact area is porportional to load.
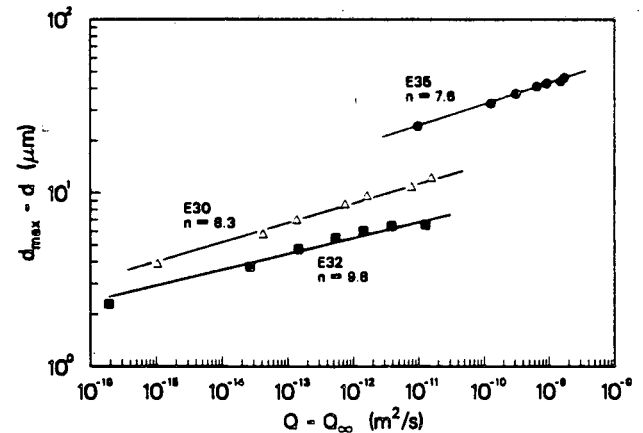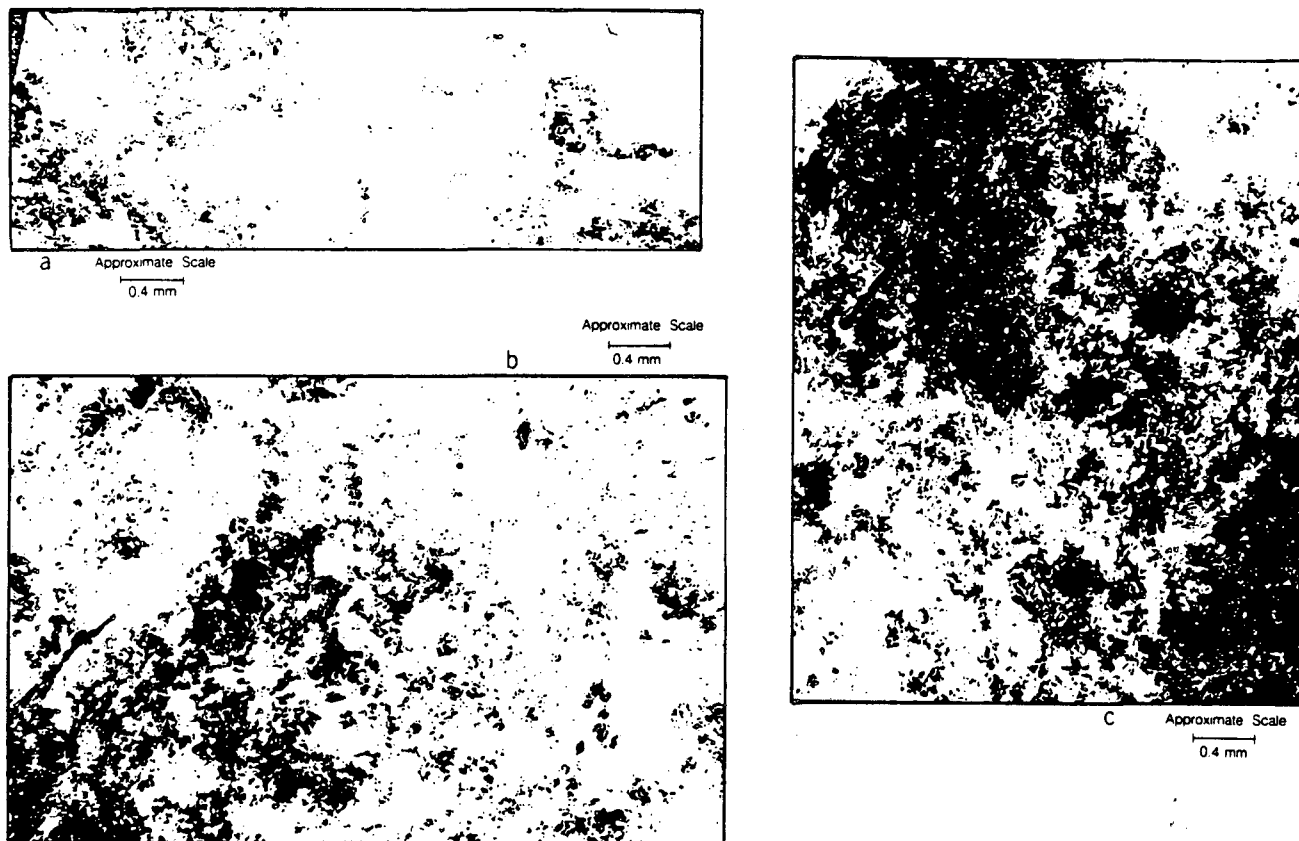

Figure 6. Fracture displacement versus flow per unit head drop for samples E35, E30, and E32.

Figure 7. Fracture displacement versus flow per unit head drop after subtraction of irreducible flow for samples E35, E30, and E32.

Figure 8. Compositve from micrographs of portion of fracture surfaces of sample E30 at three effective stresses: (a) 3 MPa; (b) 33 MPa; (c) 85 MPa (white regions are metal).

XBL 8612-4934

Although E30 shows a more or less linear relationship between stress and contact area, E32 does not; our experimental results show a nonlinear relation between specific stiffness and stress.

The increase in contact area with stress for sample E30 correlates well with observed increases in stiffness with stress. Though the stiffness of sample E32 gradually increases at higher stresses, the contact area appears to be almost constant. This suggests that the gradual increase in stiffness is due to contact at many small points not discernible on the large composite images (Figure 9).

4 DISCUSSION

Wood's metal injection tests, in combination with mechanical and hydrologic measurements, have provided clear indications of how changes in these properties with stress are related to changes in contact area and void geometry.

At low normal stresses the mechanical behavior of the fractures is characterized by nonlinear displacement and rapidly changing specific stiffness and contact area. Though the observed mechanical response could be attributed to nonlinear elastic properties, there is no evidence to suggest that hard rocks exhibit significant nonlinear elasticity. The rapid increase in specific stiffness must be caused primarily by an increase in the number of asperities coming into contact. The higher specific stiffness values for E32 than in E30 suggest a higher contact area, which is confirmed by the injection tests.

At higher stresses in samples E32 and E35, the nearly constant values of specific stiffness reflect continued elastic deformation of voids, with negligible changes in geometry or contact area. Therefore, the voids that remain open at high stresses must have aspect ratios smaller than those that would close at a stress of 85 MPa. The lower stiffness of sample E35 compared with that of the other samples is probably a result of the presence of larger voids.

For laminar flow between parallel plates, a cubic relationship exists between flow and aperture. The flow in our experiments is determined to be laminar, both from estimations of the Reynolds number and from flow experiments in which the viscosity of the fluid was changed from 1.0 cP through 1000 cP. In these experiments, flow varied inversely as the viscosity to within a few percent. Tsang (1984) determined that flow will depend on the number of small apertures and that for contact area greater than 30%, flow is greatly affected by tortuosity.

If a parallel plate model is assumed to represent the fluid flow through the fracture, the large values of n (exponent in equation (1)) determined from our experiments suggest a nonlinear relationship between mechanical displacement and hydraulic aperture. Figure 11 presents the changes in hydraulic aperture, b, calculated from the cubic law and the measured values of the mechanical displacement, d.

At low stresses, the effective hydraulic aperture changes more rapidly than is reflected by the mechanical displacement, whereas at high stresses relatively large mechanical displacements occur with little change in hydraulic aperture. This implies that at low stresses the voids through which the fluid flows close preferentially. At high stresses, the principal impediments to fluid flow must consist of tubes or orifices with equidimensional cross section that do not diminish significantly with increasing stress. Moreover, there must be significant areas of voids with apertures large enough to accommodate the mechanical displacement up to 85 MPa without closing. Presumably, these voids must be very poorly interconnected hydraulically, or else they would constitute relatively free flow paths for the fluid. Evidence to support this interpretation was provided by the metal-injection tests. At low stresses, contact area was isolated (Figure 8a) so that fluid flowed through large void areas,

5
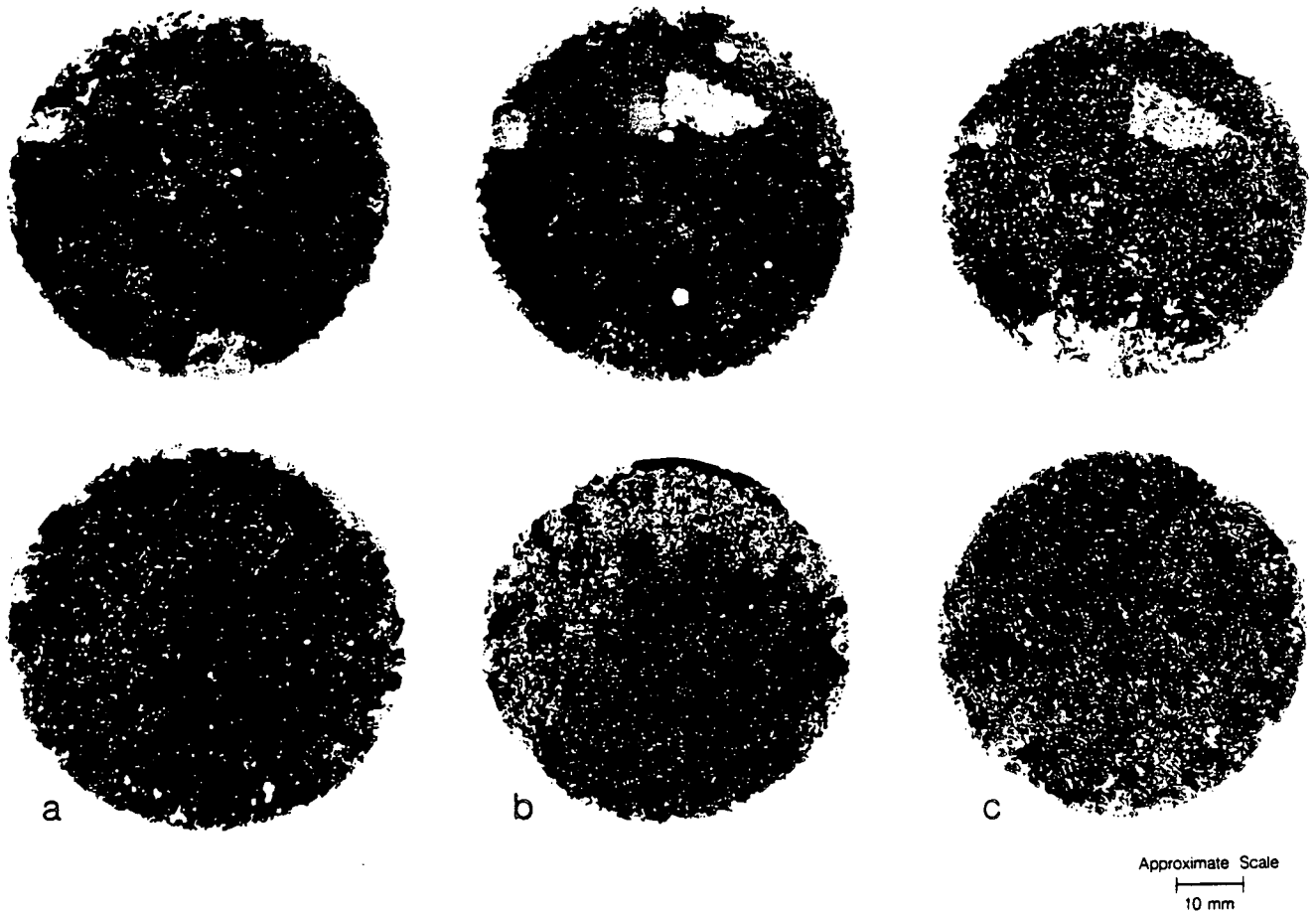
XBL 8612-4933

Figure 9. Composite photographs of entire fracture surface
of sample E30 (upper row) and E32 (lower row) at three
effective stresses: (a) 3 MPa; (b) 33 MPa; (c) 85 MPa (dark
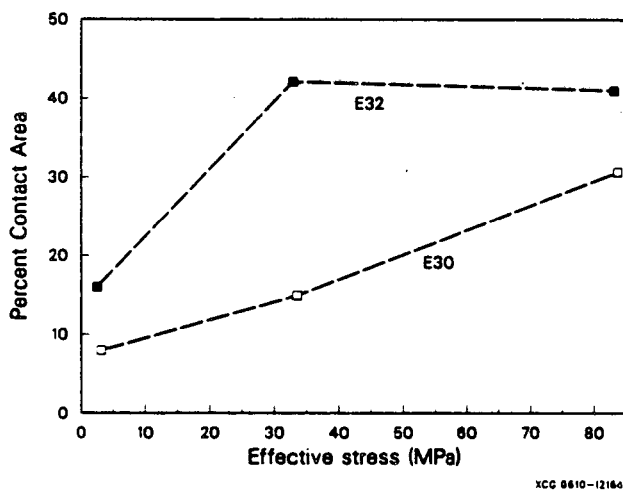regions are metal).

XCG 8610-12164

Figure 10. Contact area as a function of effective normal
stress for samples E30 and E32; results of image analysis of
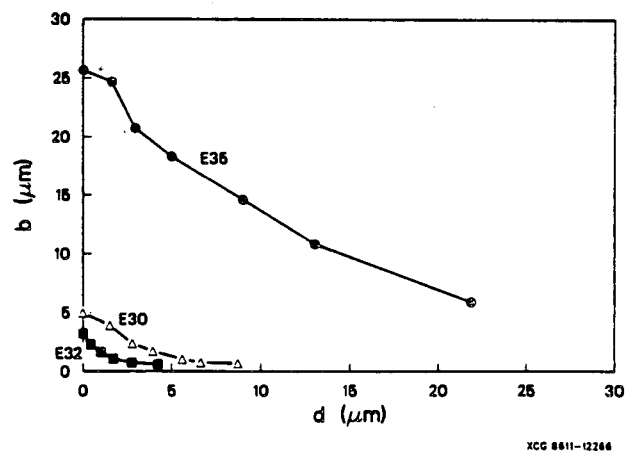photographs in Figure 9.

XCG 8611-12266

Figure 11. Calculated value of hydraulic aperture versus
measured mechanical aperture for samples E35, E30, and
E32.

6

which would also be subject to mechanical closure. At high stresses, large void areas still remained (Figure 8c) to accommodate further mechanical closure. However, the contact area was distributed such that the hydraulic connections between the voids were limited to small tortuous channels.

5 CONCLUSIONS

The hydraulic and mechanical properties of low-permeability rock are dominated by fractures. A comprehensive study of the mechanical and hydraulic behavior of natural fractures in crystalline rock under normal stress has been performed. From measurements of the mechanical displacement of a fracture, contact area of a fracture, and fluid flow through a fracture as a function stress, a clear, though qualitative, indication is given of how changes in asperity contact and void geometry affect both the mechanical and hydraulic behavior of a fracture. These results illustrate the important influence of changes in fracture geometry with increasing stress; i.e., changes in size and distribution of asperities and voids.

The cubic law relating the fluid flow through fractures in rock to the mean aperture between the fracture surfaces has been proposed on theoretical grounds. Most of the experiments that have substantiated this cubic relationship have been done either on surfaces prepared by machine or artificially induced tensile fractures. In the former case, the variability in the actual aperture because of the imperfectly planar nature of the surfaces can be expected to be small. In the latter case, the topographies of the two surfaces may be quite pronounced but the two surfaces register almost exactly, so that the apertures are everywhere very similar despite their tortuosity in the out-of-plane direction.

Natural rock fractures that have been subjected to any degree of shear motion or alteration are not only far from perfectly planar but the topographies of the opposing surfaces fail to register. Therefore, contact between natural fracture surfaces will occur at asperities, corresponding to mutual topographic highs. Surrounding the asperities will be voids, corresponding to mutual lows. Both asperities and the adjacent voids deform under increasing stress, increasing the numbers of asperities in contact and diminishing the volumes of the voids. It is these geometrical changes that result in the nonlinear displacement of a fracture with stress and the change in specific stiffness with stress. These changes can also be expected to change the apertures through which fluid flows.

The experiments reported here show that the cubic relationship between fixed flow and mechanical fracture displacement does not hold at either high or low stresses for natural fractures, as has also been found by Raven and Gale.

It is clear that the observed behavior of natural fracture surfaces must be the result of the complex relationship between the geometries of asperities in contact and the adjacent voids. This geometry is a result of the interaction between the topographies of the two fracture surfaces and their deformation under stress. This results in highly nonlinear changes in the plan areas of the voids, their apertures, and the way in which they are interconnected. Accordingly, it will be necessary to study the detailed distribution of the apertures of voids and their interconnections at different values of applied normal stress.

7 REFERENCES

Bandis, S.C., A.C. Lumsden and N.R. Barton 1983. Fundamentals of rock joint deformation. Int. J. Rock Mech. Min. Sci. Geomech. Abstr. 20(6):249—268.

Brown, S.R. and C.H. Scholz 1985. Closure of random elastic surfaces in contact. J. Geophys. Res. 90(B7):5531—5545.

Duncan, N. and K.E. Hancock 1966. The concept of contact stress in assessment of the behavior of rock masses as structural foundations. Proc. First Cong., Int. Soc. Rock Mech., Lisbon 2:487—492.

Engelder, T. and C.H. Scholz 1981. Fluid flow along very smooth joints at effective pressures up to 200 megapascals. In Mechanical behavior of crustal rocks. Am. Geophys. Union Monogr. 24:147—152.

Gale, J.E. and K.G. Raven 1980. Effects of sample size on the stress-permeability relationship for natural fractures. Lawrence Berkeley Laboratory Report, LBL-11865 (SAC-48), Berkeley, California.

Goodman, R.E. 1976. Methods of geological engineering in discontinuous rocks, p. 172. New York: West Publishing.

Greenwood, J.A. and J.B.P. Williamson 1966. Contact of nominally flat surfaces. Proc. R. Soc. London A295.

Iwai, K. 1976. Fundamentals of fluid flow through a single fracture. Ph.D. thesis, 280 p. Univ. of Calif., Berkeley.

Kranz, R.L., A.D. Frankel, T. Engelder and C.H. Scholz 1979. The permeability of whole and jointed Barre granite. Int. J. Rock Mech. Min. Sci. Geomech. Abstr. 16:225—234.

Press, W.H., B.P. Flannery, S.A. Teukolsky and W.T. Vettering 1986. Numerical recipes, p. 509. New York: Cambridge Univ. Press.

Raven, K.G. and J.E. Gale 1985. Water flow in a natural rock fracture as a function of stress and sample size. Int. J. Rock Mech. Min. Sci. Geomech. Abstr. 22(4):251—261.

Swan, G. 1983. Determination of stiffness and other joint properties from roughness measurements. Rock Mech. Rock Eng. 16:19—38.

Swanson, B.F. 1979. Visualizing pores and non-wetting phase in porous rock. J. Petrol. Tech. 31:10—18.

Tsang, Y.W. 1984. The effect of tortuosity on fluid flow through a single fracture. Water Resour. Res. 20(9):1209—1215.

Walsh, J.B. 1981. Effect of pore pressure and confining pressure on fracture permeability. Int. J. Rock Mech. Min. Sci. Geomech. Abstr. 18:429—435.

Yadav, G.D., F.A.L. Dullien, I. Chatzis and I.F. MacDonald 1984. Microscopic distribution of wetting and non-wetting phases in sandstones during immiscible displacements. SPE 13212, Society of Petroleum Engineers of AIME, Dallas, Texas.

LAWRENCE BERKELEY LABORATORY
TECHNICAL INFORMATION DEPARTMENT
UNIVERSITY OF CALIFORNIA
BERKELEY, CALIFORNIA 94720